# Optical Coherence Tomography Angiography in the Evaluation of Geographic Atrophy Area Extension

Eleonora Corbelli,[1] Riccardo Sacconi,[1,2] Alessandro Rabiolo,[1] Stefano Mercuri,[1] Adriano Carnevali,[1,3] Lea Querques,[1] Francesco Bandello,[1] and Giuseppe Querques[1]

[1]Department of Ophthalmology, University Vita-Salute, IRCCS Ospedale San Raffaele, Milan, Italy
[2]Eye Clinic, Department of Neurological, Biomedical and Movement Sciences, University of Verona, Verona, Italy
[3]Department of Ophthalmology, Magna Graecia University, Catanzaro, Italy

Correspondence: Giuseppe Querques, Department of Ophthalmology, University Vita-Salute, IRCCS Ospedale San Raffaele, Via Olgettina 60, Milan, 20132, Italy; giuseppe.querques@hotmail.it.

Submitted: June 28, 2017
Accepted: September 15, 2017

Citation: Corbelli E, Sacconi R, Rabiolo A, et al. Optical coherence tomography angiography in the evaluation of geographic atrophy area extension. *Invest Ophthalmol Vis Sci*. 2017;58:5201–5208. DOI:10.1167/iovs.17-22508

**Purpose.** To investigate the application of optical coherence tomography angiography (OCT-A) in evaluation of geographic atrophy (GA) secondary to age-related macular degeneration (AMD).

**Methods.** Patients with GA were prospectively enrolled and studied with blue fundus autofluorescence (FAF), en face structural OCT, and OCT-A. OCT-A images were acquired using a slab of whole choroid, whereas en face structural OCT images were obtained at the ellipsoid zone (EZ), at the choroidal (CH) level, and at the scleral (SC) level. Three readers independently measured the GA extension areas and evaluated the foveal sparing in each examination. Intraobserver/interobserver agreements and agreement between each couple of imaging techniques were assessed.

**Results.** A total of 47 eyes (26 patients, mean age 76 ± 7 years) with GA (mean area using FAF: 8.77 ± 5.00 $mm^2$) were included. Intraobserver and interobserver agreement was excellent for all imaging techniques (intraclass correlation coefficient [ICC] > 0.985), even if en face EZ structural OCT revealed the poorest quality agreement limits. Considering the analysis between each couple of imaging techniques, ICC was excellent between OCT-A compared with FAF (ICC: 0.995), followed by en face structural OCT at CH level (ICC: 0.992), at SC level (ICC: 0.986), and at EZ level (ICC: 0.973). No differences were detected between multifocal and monofocal GA lesions. Considering the evaluation of foveal involvement, lower agreements were disclosed between FAF and all other imaging techniques.

**Conclusions.** OCT-A is a reliable technique for easily visualizing and quantifying GA with the advantages, compared to current imaging techniques, of offering together both structural and blood flow information regarding retinal and choroidal layers and excluding choroidal neovascularization.

Keywords: age-related macular degeneration, fundus autofluorescence, en face optical coherence tomography, geographic atrophy, optical coherence tomography angiography

Geographic atrophy (GA), the advanced form of dry age-related macular degeneration (d-AMD), represents an important unmet need with more than 5 million people worldwide affected.[1] In contrast to neovascular AMD, the other form of late AMD, characterized by sudden and rapid central vision loss due to new abnormal blood vessels, GA is a slow disease leading to irreversible blindness over years.[2,3] The morphologic changes in GA area represented by degeneration of photoreceptor cells, retinal pigment epithelium (RPE), and choriocapillaris (CC) initially appear in the extrafoveal region and then include the fovea,[2,3] with limitations in key aspects of daily life.[4] Previous studies have reported an atrophic lesion growth rate between 1.3 and 2.8 $mm^2$ per year.[2,5,6]

To follow up the GA enlargement over time, it is critical to measure the size of the atrophy and to identify methods providing reliable measurements. GA is usually assessed by color fundus photography (CFP)[7] and fundus autofluorescence (FAF), currently considered the gold standard for evaluating progressive atrophy enlargement.[8,9] However, GA can be reproducibly identified and quantified by means of various other modalities available in daily clinical practice. Ben Moussa et al.[10] demonstrated that multicolor imaging is an excellent tool for measuring GA area and for detecting foveal sparing, although structural optical coherence tomography (OCT) showed the highest intergrader agreement on foveal sparing detection when compared to several different procedures.[11,12] OCT imaging offers also the advantage of providing an en face image of GA as complement of B-scan cross-sectional images. Pilotto et al.[13] revealed that in patients with GA the abrupt transition in OCT reflectivity caused by photoreceptor loss results in the visualization of GA on outer retina (OR) en face OCT images, whereas the increased OCT choroidal signal associated with GA allows visualization of atrophic areas on choroidal (CH) en face OCT images.

More recently, the development of OCT angiography (OCT-A) has allowed detection of GA as loss of CC flow under the atrophic patches with improved visualization of CH vessels.[14] In fact, this technique maps the movement of red blood cells relative to the static surrounding tissue, thus creating an image of vascular flow. However, to the best of our knowledge, no

published studies have evaluated the ability of OCT-A to quantify GA size.

In this study we assessed intraobserver and interobserver agreement in detection and quantification of GA secondary to d-AMD using OCT-A. Moreover, we compared OCT-A, FAF, and en face OCT imaging modalities in order to identify the most reproducible method for monitoring GA progression and for evaluating potential therapeutic responses in clinical trials.

## Methods

We prospectively enrolled consecutive patients with diagnosis of GA secondary to d-AMD who presented at the Medical Retina & Imaging Unit of the Department of Ophthalmology, University Vita-Salute, San Raffaele Hospital in Milan, between August 2016 and February 2017. This study adhered to the tenets of the Declaration of Helsinki. All patients signed a written informed consent to participate in observational studies, approved by the ethics committee of San Raffaele Hospital.

The criteria for inclusion were (1) age greater than 55 years, (2) diagnosis of d-AMD with GA (GA was defined as any sharply demarcated monofocal or multifocal area of apparent absence of the RPE measuring at least 175 μm in greatest linear diameter within the macula, with visible CH vessels and no neovascularization). The exclusion criteria were (1) signs of choroidal neovascularization (CNV), including intraretinal or subretinal fluid, hemorrhage, subretinal fibrosis; (2) presence of any other retinal disorders potentially confounding the clinical assessment (e.g., diabetic retinopathy, retinal vein occlusion, retinal artery occlusion); (3) myopia greater than 6 diopters; (4) any previous treatments (e.g., laser photocoagulation, photodynamic therapy, intravitreal injections of anti-vascular endothelial growth factors or steroids); (5) presence of significant media opacities (e.g., cataract or corneal opacity) (to ensure proper image quality). Patients were also excluded if the GA extended outside the central scanning area, which was a square centered on the fovea with dimensions of $6 \times 6$ mm.

All patients underwent a complete ophthalmologic examination, including best-corrected visual acuity (BCVA) using Early Treatment Diabetic Retinopathy Study (ETDRS) charts, slit-lamp biomicroscopy, tonometry, indirect fundus ophthalmoscopy, infrared reflectance (IR), FAF, spectral-domain OCT (SD-OCT), fluorescein angiography (FA), indocyanine green angiography (ICGA), and OCT-A scans of the macula. IR, FAF, SD-OCT, FA, and ICGA were performed using Spectralis (Heidelberg Engineering, Heidelberg, Germany). To achieve good visualization of the choroid, enhanced depth imaging (EDI) OCT was used in all acquisitions. All patients underwent all imaging acquisition on the same day.

### Image Acquisition

Blue FAF was performed with confocal scanning laser ophthalmoscope (SLO) system using Spectralis (excitation: 488 nm; emission: 500–700 nm) in a field of view of $30° \times 30°$ centered on the macula. The automatic real-time averaging mode (ART) was enabled to obtain averaged scans. For the study, the ART was set at 100 frames to obtain best quality of FAF.

En face structural OCT and OCT-A were performed with AngioPlex (Cirrus HD-OCT model 5000; Carl Zeiss Meditec, Dublin, CA, USA). We used a $6 \times 6$-mm scanning area centered on the macula, which is composed of 350 A-scans in each B-scan, repeated two times, along both the horizontal and the vertical direction. All acquisitions were performed using FastTrac retinal-tracking technology to reduce motion artifacts. Minimum strength of OCT-A images was 7 out of 10. Using the automatic segmentation of the device, we selected three different en face structural OCT images: the ellipsoid zone (EZ), the choroidal (CH) images, and the scleral (SC) images. The en face EZ image was obtained considering a segmentation reference of 21 μm in depth passing 45 μm above the RPE (Fig. 1, first image). The en face CH image was obtained considering a segmentation reference line passing from 29 μm below the RPE and the chorio-scleral interface (Fig. 1, second image). The en face SC image was obtained considering a segmentation reference line passing from 29 μm below the RPE and arbitrary 350 μm below the RPE (Fig. 1, third image). Image segmentation was manually adjusted by the senior author (GQ) if the automatic segmentation failed.

Considering OCT-A images, we used a slab of the whole choroid (CC, Sattler and Haller's layers), which was manually defined by the senior author (GQ) as the vertical distance between the hyperreflective line of the RPE (by selecting the "RPE fit" option on AngioPlex) and the chorio-scleral interface (Fig. 1, fourth image).

### Image Analysis

For each eye, the GA area was measured by three independent readers. The three readers independently measured, at two different times, the area affected by GA on each image.

All FAF, en face EZ, en face CH, en face SC, and OCT-A images were exported into Image J 1.50 (National Institutes of Health, Bethesda, MD, USA) software. The atrophic area was manually outlined using the polygon selection tool in each image. In FAF, sharply demarcated areas of reduced autofluorescence were considered the atrophic area, which could be surrounded by a hyperautofluorescent outer border. In en face structural OCT, sharply demarcated areas of altered pigmentation of EZ and/or RPE that could be associated with improved visualization of the CH vasculature were defined as the atrophic area (Fig. 1, first through third images). In OCT-A, the areas of lack of CC with improved visualization of the CH vasculature were considered the atrophic area (Fig. 1, fourth image).

Total GA area was calculated for each image by summing all the areas of GA. Areas corresponding to drusen were not included. To measure the GA, pixel area was converted into square millimeters ($mm^2$) according to the scale of the image. After processing every atrophic area measure, screenshot and report were generated and recorded for analysis. When grading one image, each reader was blind to all other images from the same patient.

Secondarily, all GA were classified as in monofocal or multifocal atrophy, and as in foveal sparing or foveal involvement atrophy according to the presence or absence of a foveal involvement. To evaluate the presence of foveal sparing/involvement, the three readers independently evaluated the presence of foveal sparing in GA on FAF, en face EZ, en face CH, en face SC, and OCT-A.

### Statistical Analysis

Statistical analyses were performed using SPSS Statistics Version 20 (IBM; Armonk, New York, NY, USA). Results of descriptive analyses are expressed as means ± standard deviations for quantitative variables, and as counts and percentages for categorical variables. The Gaussian distribution of continuous variables was verified with the Kolmogorov-Smirnov test. Comparisons of mean area and mean differences of GA areas were performed using Student's independent samples *t*-test. Intraobserver and interobserver agreements,

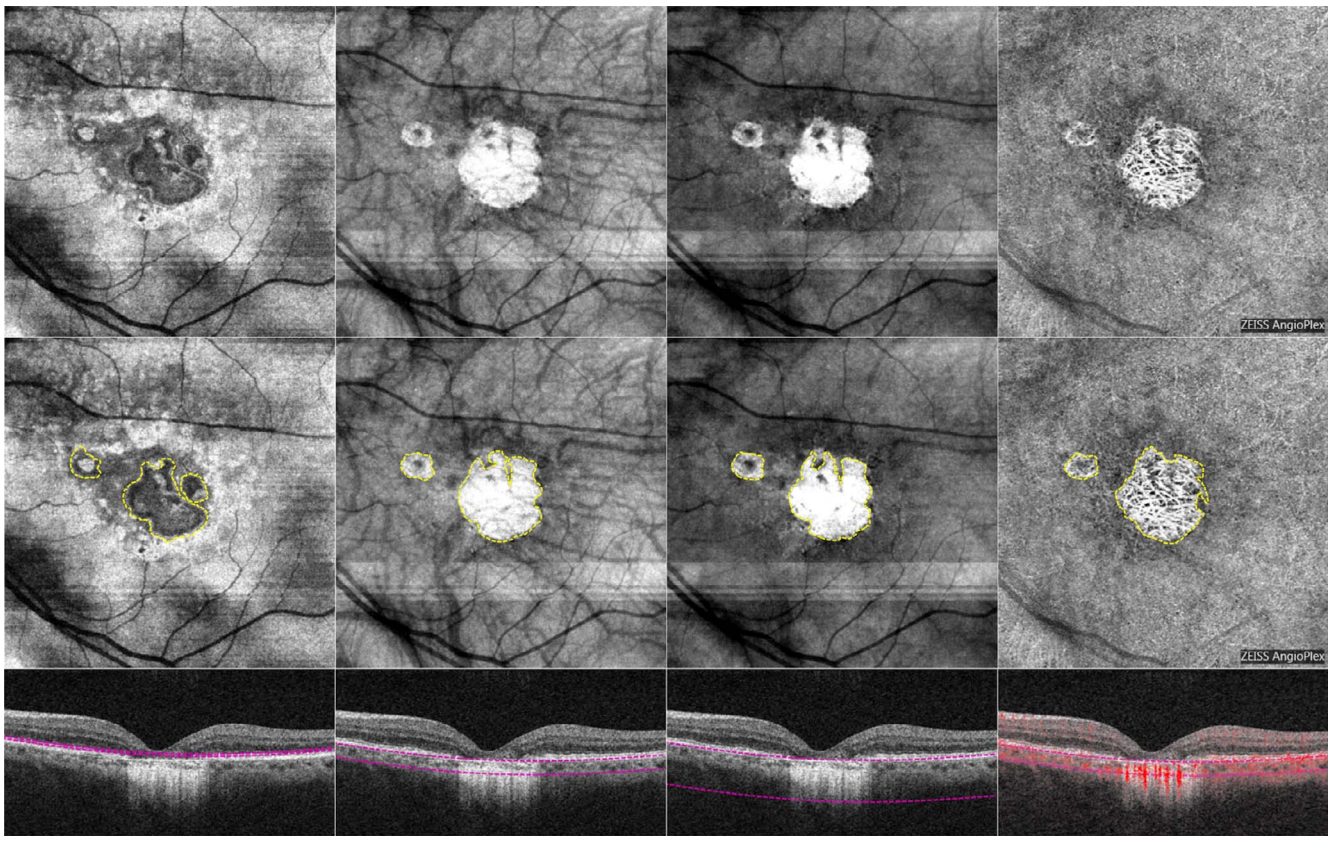


FIGURE 1. En face structural optical coherence tomography (OCT) at the ellipsoid zone (first image), choroidal (second image), and scleral (third image) layer level and OCT angiography (fourth image) without and with the demarcation lines of geographic atrophy areas (*first and second row*, respectively). Corresponding structural B-scans (*third row*) showing the segmentation lines used to obtain the en face images.

and the correlation between FAF, en face EZ, en face CH, en face SC, and OCT-A, were evaluated using the intraclass correlation coefficient (ICC; 95% confidence intervals [CI]). Furthermore, Bland-Altman plots were constructed to determine the limits of agreement. A range of ±15% of FAF mean values was assumed as interval of clinical equivalence as reported in previous studies.[13] We accepted the equivalence assessment if the 95% agreement limits of the difference between the mean values of two different imaging techniques resulted completely within the equivalence interval. To quantify interobserver agreement concerning the foveal involvement or sparing, a Cohen's Kappa ($\kappa$) coefficient was calculated. In all analyses, $P$ values $< 0.05$ were considered statistically significant.

## RESULTS

Forty-seven eyes of 26 patients (17 females, 9 males) met the inclusion criteria and were included for the analysis. The fellow eyes of 5 patients were not included in the analysis due to the presence of a neovascular AMD (three eyes) or improper image quality (two eyes). The mean age was 76 ± 7 years (median, 76.5; range, 65–87), and the ethnicity was Caucasian for all patients. By means of FAF, the mean area of GA lesion was 8.77 ± 5.00 mm$^2$ (range, 1.45–22.47), compared to 8.86 ± 5.01 mm$^2$ (range, 1.30–22.56 [$P = 0.930$]) using en face EZ; 8.62 ± 4.90 mm$^2$ (range, 1.60–23.16 [$P = 0.884$]) using en face CH; 8.55 ± 4.85 mm$^2$ (range, 1.60–23.04 [$P = 0.833$]) and 8.75 ± 4.96 mm$^2$ (range, 1.44–22.59 [$P = 0.989$]) using OCT-A (Table 1). Among the 47 eyes analyzed, a monofocal atrophic lesion was disclosed in 15 eyes, whereas the atrophic lesion was multifocal in the other 32 eyes (Fig. 2).

### Intraobserver Agreement

Using FAF, intraobserver repeatability was excellent (ICC = 0.998 [95% CI, 0.997–0.999]). On en face structural OCT, intraobserver repeatability was excellent at the level of the EZ, at the CH level, and at the SC level (ICC = 0.998 [95% CI, 0.997–0.999], ICC = 0.999 [95% CI, 0.998–0.999], and ICC = 0.995 [95% CI, 0.992–0.997], respectively). Also by means of OCT-A, intraobserver was excellent (ICC = 0.999 [95% CI, 0.998–0.999]). The construction of Bland-Altman plots confirmed the great intraobserver agreement for all imaging techniques (Supplementary Fig. S1). No differences in intraobserver agreement were detected between multifocal and monofocal lesions ($P > 0.05$ in all analyses).

### Interobserver Agreement

The interobserver reliability between readers 1, 2, and 3 was assessed in two different ways. First, ICC coefficients were calculated. The interobserver agreement for readers 1, 2 and 3 was excellent for all image acquisitions: ICC 0.997 (95% CI, 0.995–0.998) for FAF, ICC 0.986 (95% CI, 0.978–0.992) for en face EZ structural OCT, ICC 0.996 (95% CI, 0.994–0.998) for en face CH structural OCT, ICC 0.994 (95% CI, 0.990–0.996) for en face SC structural OCT, and ICC 0.996 (95% CI, 0.993–0.998) for en face OCT-A. The second measure of interobserver reliability involved the construction of Bland-Altman plots. All mean differences by readers, standard deviations, and agreement limits calculated to construct Bland-Altman plots are

**Table 1.** Measurement of Geographic Atrophy in FAF, En Face EZ, CH, and SC Structural OCT and OCT-A

| | | Area | | | |
|---|---|---|---|---|---|
| **Measurement Method** | **Observer** | **Mean, mm²** | **Standard Deviation, mm²** | **Minimum, mm²** | **Maximum, mm²** |
| FAF | Mean | 8.77 | 5.00 | 1.45 | 22.47 |
| | 1 | 8.79 | 5.00 | 1.21 | 22.55 |
| | 2 | 8.75 | 4.93 | 1.59 | 22.28 |
| | 3 | 8.76 | 5.09 | 1.18 | 22.58 |
| En face EZ | Mean | 8.86 | 5.01 | 1.30 | 22.56 |
| | 1 | 8.86 | 5.00 | 1.40 | 22.18 |
| | 2 | 8.90 | 5.02 | 1.22 | 23.29 |
| | 3 | 8.81 | 5.08 | 1.20 | 22.21 |
| En face CH | Mean | 8.62 | 4.90 | 1.60 | 23.16 |
| | 1 | 8.61 | 4.87 | 1.49 | 22.85 |
| | 2 | 8.67 | 4.96 | 1.64 | 23.10 |
| | 3 | 8.57 | 4.96 | 1.50 | 23.53 |
| En face SC | Mean | 8.55 | 4.85 | 1.60 | 23.04 |
| | 1 | 8.58 | 4.81 | 1.51 | 22.80 |
| | 2 | 8.61 | 4.87 | 1.69 | 22.99 |
| | 3 | 8.46 | 4.89 | 1.60 | 23.33 |
| OCT-A | Mean | 8.75 | 4.96 | 1.44 | 22.59 |
| | 1 | 8.71 | 4.89 | 1.43 | 22.07 |
| | 2 | 8.82 | 4.98 | 1.47 | 22.89 |
| | 3 | 8.71 | 5.02 | 1.31 | 22.82 |

reported in Table 2. As shown in Supplementary Figure S2, interobserver reliability between each pair of readers was corroborated by Bland-Altman plots for all image acquisitions. Even though all imaging techniques showed a good agreement with a maximum mean difference of 0.114 mm², en face EZ structural OCT revealed poor-quality agreement limits (see Supplementary Fig. S2). No differences in interobserver agreement were detected between multifocal and monofocal lesions ($P > 0.05$ in all analyses). The interobserver agreement considering the evaluation of foveal involvement was excellent between all graders for all the imaging techniques used ($\kappa >$ 0.8 with concordant pairs > 96% in all analyses; Table 3).

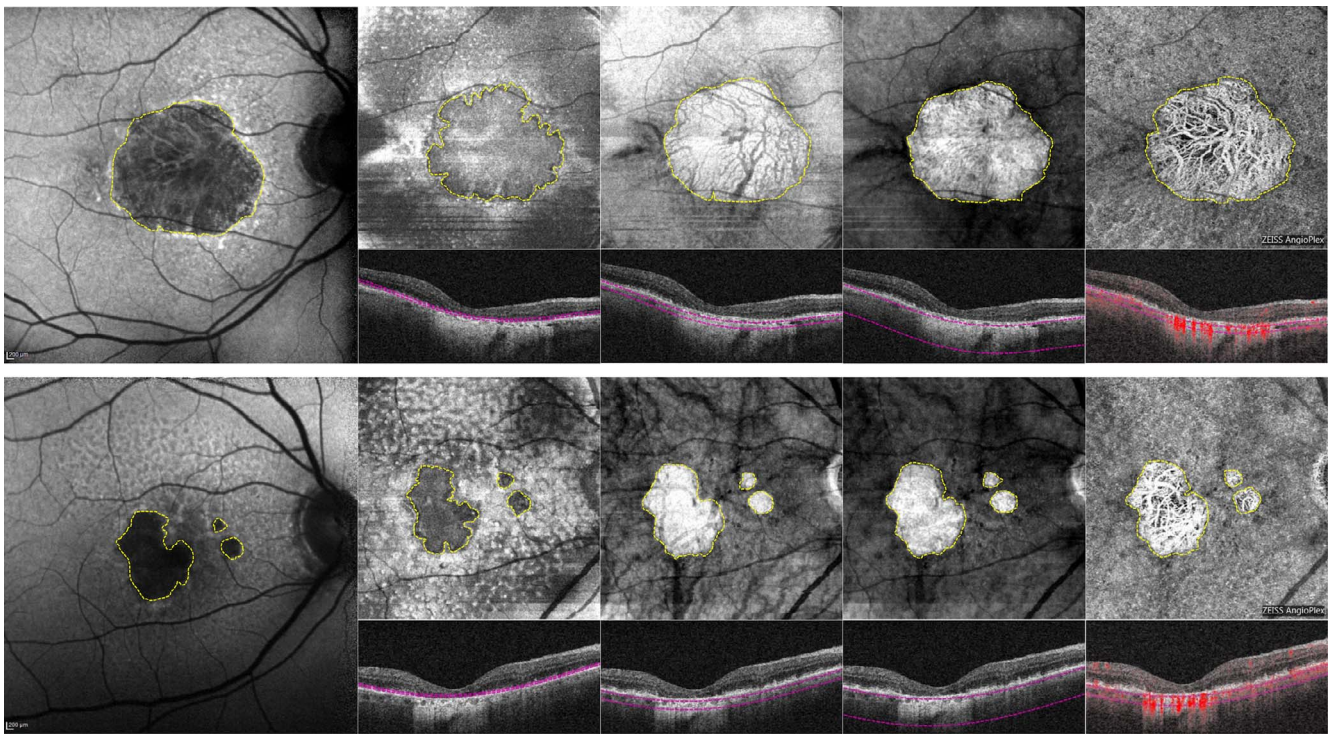


**Figure 2.** In the *first row*, right eye of a 75-year-old woman with monofocal geographic atrophy (GA) imaged using different modalities and measured manually on fundus autofluorescence (first image), en face optical coherence tomography (OCT) at the ellipsoid zone (second image), choroidal (third image), and scleral (fourth image) layer level and OCT angiography (fifth image). *Second row* shows right eye of an 84-year-old man with multifocal GA imaged using different modalities and measured manually on fundus autofluorescence (first image), en face OCT at the ellipsoid zone (second image), choroidal (third image), scleral (fourth image) layer level, and OCT angiography (fifth image).

**Table 2.** Mean Differences in Geographic Atrophy Measurements by Readers, Standard Deviations, and Agreement Limits Using FAF, En Face EZ, CH, and SC Structural OCT and OCT-A

| Measurements | Observers | Mean Difference, mm$^2$ | Standard Deviation, mm$^2$ | Agreement Limits, 95% | |
|---|---|---|---|---|---|
| | | | | Lower Limit | Upper Limit |
| FAF | 1, 2 | 0.044 | 0.305 | −0.551 | 0.640 |
| | 1, 3 | 0.039 | 0.434 | −0.808 | 0.885 |
| | 2, 3 | −0.006 | 0.432 | −0.849 | 0.837 |
| En face EZ | 1, 2 | −0.038 | 0.854 | −1.702 | 1.627 |
| | 1, 3 | 0.046 | 0.971 | −1.847 | 1.940 |
| | 2, 3 | 0.084 | 0.662 | −1.206 | 1.374 |
| En face CH | 1, 2 | −0.056 | 0.379 | −0.796 | 0.683 |
| | 1, 3 | 0.035 | 0.444 | −0.830 | 0.900 |
| | 2, 3 | 0.092 | 0.414 | −0.716 | 0.899 |
| En face SC | 1, 2 | −0.023 | 0.435 | −0.871 | 0.825 |
| | 1, 3 | 0.119 | 0.564 | −0.980 | 1.219 |
| | 2, 3 | 0.142 | 0.595 | −1.018 | 1.302 |
| OCT-A | 1, 2 | −0.112 | 0.385 | −0.863 | 0.640 |
| | 1, 3 | 0.002 | 0.458 | −0.892 | 0.896 |
| | 2, 3 | 0.114 | 0.473 | −0.808 | 1.036 |

### Correlation Between FAF, En Face Structural OCT (EZ, CH, and SC), and OCT-A Images

As for interobserver reliability, the correlation between different imaging techniques was also evaluated in two ways. First, ICC coefficients were calculated. Mean GA area measured on FAF better correlated to GA area measured on OCT-A (ICC 0.995; 95% CI, 0.991–0.997) followed by en face structural OCT at the CH level (ICC 0.992; 95% CI, 0.986–0.996) and en face structural OCT at the SC level (ICC 0.986; 95% CI, 0.975–0.992). Interclass correlation coefficient was excellent also between en face structural OCT at the CH level compared with OCT-A (ICC 0.992; 95% CI, 0.986–0.996) and with en face structural OCT at the SC level (ICC 0.995; 95% CI, 0.992–0.997). Even if excellent, en face EZ structural OCT showed the lowest ICC with FAF (ICC 0.973; 95% CI, 0.952–0.985), with en face CH structural OCT (ICC 0.974; 95% CI, 0.954–0.986), with en face SC structural OCT (ICC 0.964; 95% CI, 0.936–0.980), and with OCT-A (ICC 0.975; 95% CI, 0.957–0.986). The second measure of correlation between each couple of imaging techniques involved the construction of Bland-Altman plots (see Supplementary Fig. S3). Table 4 summarizes all mean differences by imaging techniques, standard deviations, and agreement limits calculated to construct Bland-Altman plots. Also this analysis confirmed good agreement between each imaging technique: The mean differences between measurements of GA area using different techniques were close to zero for each eye, with a maximum mean difference of 0.307 mm$^2$ between en face structural OCT at the level of EZ and en face structural OCT at the SC level. As shown in Table 4 and Supplementary Figure S3, the lowest agreement limits were disclosed between FAF and en face EZ and between en face EZ and en face SC. No differences in agreement between FAF, en face structural OCT (EZ, CH, and SC), and OCT-A were detected between multifocal and monofocal lesions ($P > 0.05$ in all analyses) (Fig. 2).

Considering the evaluation of foveal involvement, the correlation between different imaging techniques was good/excellent between all imaging techniques analyzed (Table 5). Lower agreements were disclosed between FAF and all other imaging techniques (en face structural OCT [EZ, CH, and SC] and en face OCT-A). In almost all discordant cases, the fovea seemed to be involved with FAF imaging while it seemed to be spared with other imaging techniques (Fig. 3).

## Discussion

In this study, we evaluated the reliability of OCT-A for detecting and quantifying GA secondary to d-AMD. Moreover, we compared measurements obtained by three readers using OCT-A, FAF, and en face OCT. Similar to previous studies evaluating CFP, FAF, structural OCT, and en face OCT,[11,13,15–19] our analysis revealed high intraobserver and interobserver

**Table 3.** Mean Differences in Geographic Atrophy Measurements, Standard Deviations, and Agreement Limits Between FAF, En Face EZ, CH, and SC Structural OCT, and OCT-A

| Comparison Between Measurement Methods | Mean Difference, mm$^2$ | Standard Deviation, mm$^2$ | Agreement Limits, 95% | |
|---|---|---|---|---|
| | | | Lower Limit | Upper Limit |
| FAF – en face EZ | −0.091 | 1.176 | −2.386 | 2.203 |
| FAF – en face CH | 0.150 | 0.599 | −1.019 | 1.319 |
| FAF – en face SC | 0.215 | 0.803 | −1.351 | 1.781 |
| FAF – OCT-A | 0.014 | 0.494 | −0.949 | 0.976 |
| En face EZ – en face CH | 0.242 | 1.108 | −1.919 | 2.403 |
| En face EZ – en face SC | 0.307 | 1.307 | −2.242 | 2.856 |
| En face EZ – OCT-A | 0.105 | 1.110 | −2.059 | 2.270 |
| En face CH – en face SC | 0.065 | 0.465 | −0.842 | 0.972 |
| En face CH – OCT-A | −0.136 | 0.608 | −1.321 | 1.049 |
| En face SC – OCT-A | −0.201 | 0.745 | −1.654 | 1.252 |

Table 4. Interobserver Agreement Considering the Evaluation of Foveal Involvement

| Measurement Method | Observers | κ Coefficient | Concordant Pairs (%) |
|---|---|---|---|
| FAF | 1, 2 | 0.888 | 45/47 (96) |
| | 1, 3 | 0.882 | 45/47 (96) |
| | 2, 3 | 0.882 | 45/47 (96) |
| En face EZ | 1, 2 | 0.952 | 46/47 (98) |
| | 1, 3 | 1 | 47/47 (100) |
| | 2, 3 | 0.952 | 46/47 (98) |
| En face CH | 1, 2 | 0.950 | 46/47 (98) |
| | 1, 3 | 1 | 47/47 (100) |
| | 2, 3 | 0.950 | 46/47 (98) |
| En face SC | 1, 2 | 0.950 | 46/47 (98) |
| | 1, 3 | 1 | 47/47 (100) |
| | 2, 3 | 0.950 | 46/47 (98) |
| OCT-A | 1, 2 | 0.952 | 46/47 (98) |
| | 1, 3 | 1 | 47/47 (100) |
| | 2, 3 | 0.952 | 46/47 (98) |

agreement in the evaluation of GA for CH slab OCT-A, FAF and en face OCT at the EZ, CH, and SC level.

Currently, interest in OCT-A imaging has increased because it is a fast, safe, noninvasive method able to provide higher-quality images of the retinal and CH microvasculature compared with conventional dye angiography.[20] At OCT-A evaluation, GA eyes showed loss[21] or rarefaction[14] of CC in correspondence with RPE atrophy (Figs. 1–3). In these areas of CC impairment, large CH vessels may be displaced and may be seen on the en face OCT-A image at the depth level where CC is ordinarily seen.[14] However, to the best of our knowledge, no published study has investigated the ability of OCT-A to measure GA. In the present study, we found high intragrader and intergrader agreement for GA area measured by OCT-A, which is equivalent to FAF and en face structural OCT at the CH and SC levels (Tables 1, 2; Supplementary Figs. S1, S2). One explanation of the excellent agreement found for en face OCT at the CH and SC could be their ability to increase contrast between atrophic and healthy retina. Even though en face EZ structural OCT was excellent in measuring GA, we recorded the poorest-quality interobserver agreement limits (Table 2; Supplementary Fig. S2). The inferior intergrader agreement could be explained, at least in part, by the major difficulty in segmenting and interpreting images of en face OCT at the EZ level, probably due to the very low EZ thickness.

Regarding GA measurements by OCT-A compared with FAF and en face structural OCT, the greatest correlation was found between FAF, en face OCT at the CH and SC levels, and OCT-A (Table 3; Supplementary Fig. S3). This seems in disagreement with the results reported by Pilotto et al.[13] They found a good correlation between en face structural OCT images at the OR level, both on blue FAF and on near-infrared FAF, but inconsistent correlation between FAF images and en face OCT at the CH level. However, a comparison between the two studies is not possible because different slab segmentations were investigated, with two different devices. In our study all the imaging techniques compared with OCT-A were equivalent (the difference between the GA areas measured by two different imaging techniques resulted completely within the interval of clinical equivalence) except for en face OCT at the EZ. In fact, en face OCT at the EZ level was the method not only with the lowest intergrader agreement but also with minor correlation with other techniques.

Recently, our group demonstrated a CC rarefaction in areas bordering GA using OCT-A[22] (Querques G, personal communications, Fifth Annual International Retinal Imaging Symposium (IRIS), Los Angeles, CA, USA, March 25, 2017); however, such rarefaction (not a complete absence of CC) and higher visibility of CH vessels seem not to affect the sharp visualization and delimitation of GA on OCT-A, as we did not find differences in GA areas between FAF and OCT-A CH slab. Moreover, as noted with previous studies,[16,23] FAF could potentially overestimate GA area as compared to other imaging modalities when atrophic patches are continuous with the fovea. The reason could be the inclusion of normal fovea due to the decreased foveal autofluorescence caused by increased quantity of pigments. Thus, as shown in our analysis, in these cases the fovea seemed to be involved with GA on FAF, while OCT-A and en face OCT were superior for demonstrating foveal sparing (Table 5; Fig. 3).

Table 5. Agreement Between Different Measurement Methods Considering the Evaluation of Foveal Involvement

| Comparison Between Measurement Methods | Observer | κ Coefficient | Concordant Pairs (%) |
|---|---|---|---|
| FAF – en face EZ | 1 | 0.845 | 44/47 (94) |
| | 2 | 0.798 | 43/47 (91) |
| | 3 | 0.731 | 42/47 (89) |
| FAF – en face CH | 1 | 0.894 | 45/47 (96) |
| | 2 | 0.741 | 42/47 (89) |
| | 3 | 0.778 | 43/47 (91) |
| FAF – en face SC | 1 | 0.894 | 45/47 (96) |
| | 2 | 0.741 | 42/47 (89) |
| | 3 | 0.778 | 43/47 (91) |
| FAF – OCT-A | 1 | 0.845 | 44/47 (94) |
| | 2 | 0.798 | 43/47 (91) |
| | 3 | 0.731 | 42/47 (89) |
| En face EZ – en face CH | 1 | 0.950 | 46/47 (98) |
| | 2 | 0.952 | 46/47 (98) |
| | 3 | 0.950 | 46/47 (98) |
| En face EZ – en face SC | 1 | 0.950 | 46/47 (98) |
| | 2 | 0.952 | 46/47 (98) |
| | 3 | 0.950 | 46/47 (98) |
| En face EZ – OCT-A | 1 | 1 | 47/47 (100) |
| | 2 | 1 | 47/47 (100) |
| | 3 | 1 | 47/47 (100) |
| En face CH – en face SC | 1 | 1 | 47/47 (100) |
| | 2 | 1 | 47/47 (100) |
| | 3 | 1 | 47/47 (100) |
| En face CH – OCT-A | 1 | 0.950 | 46/47 (98) |
| | 2 | 0.952 | 46/47 (98) |
| | 3 | 0.950 | 46/47 (98) |
| En face SC – OCT-A | 1 | 0.950 | 46/47 (98) |
| | 2 | 0.952 | 46/47 (98) |
| | 3 | 0.950 | 46/47 (98) |

Of note, in our study the mean difference in GA area measured by two different techniques was always under 0.50 $mm^2$ (Table 3), a value substantially lower than the atrophic lesion growth rate between 1.3 and 2.8 $mm^2$ per year reported in different natural history studies.[2,5,6] Interestingly, multifocal lesions were not a cause of lower intraobserver/interobserver agreement or of lower agreement between two different imaging techniques (Fig. 2).

Overall, based on our findings, OCT-A could be considered a reliable method to detect and quantify GA and to evaluate foveal involvement. One can argue that often OCT-A images are deteriorated with artifacts and segmentation errors in patients affected by GA. However, in our study, eye-tracker was enabled

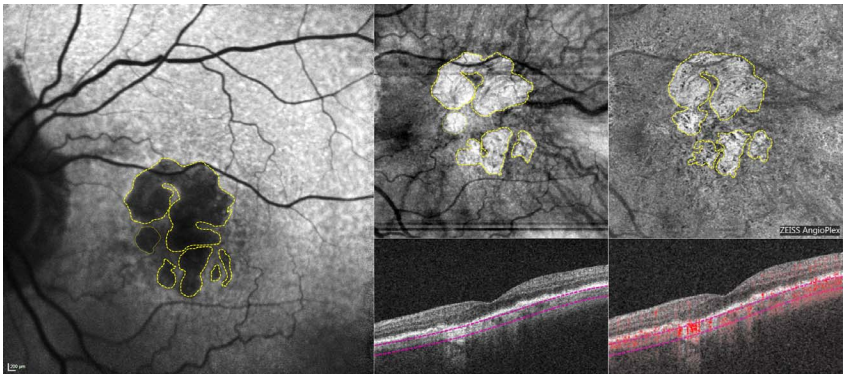

FIGURE 3. Left eye of a 76-year-old man with multifocal geographic atrophy (GA) imaged using different modalities. With fundus autofluorescence (first image), the normal hypofluorescence area corresponding to the fovea is easily confused with atrophic patch, possibly leading the examiner to classify the lesion as foveal involvement. In contrast, nonfovea involving GA is well evident by means of en face OCT at the choroidal level (second image) and optical coherence tomography angiography (OCT-A) at choroidal slab (third image).

in all acquisitions to reduce motion artifacts. Regarding the segmentation errors, we used a slab manually defined by a senior author (GQ) including the whole choroid (Figs. 1–3). This manual segmentation resolved most segmentation errors provided by the automatic segmentation of OCT-A software and highlights the areas where the CC is absent (showing only the presence of large CH vessels). However, sometimes OCT-A software completely failed in segmentation of the retinal and CH layers, leading to low-quality OCT-A images; in this condition, segmentation errors could be resolved only by a total manual time-consuming process, currently available only for some commercial OCT-A software. By excluding these cases and improving OCT-A software, we predict that OCT-A would be a practical, fast, and reliable tool to evaluate GA in clinical practice. Benefits of using OCT-A compared with other imaging approaches for GA include the convenience of using only one type of imaging technique for showing en face flow images and structural OCT data, better definition of foveal impairment compared to blue FAF, and the potential ability to exclude presence of CNV without performing FA, particularly treatment-naïve quiescent type 1 CNV.[24–26] In addition, OCT-A is not affected by some limits and disadvantages of traditional techniques. For example, even if FAF, noninvasively mapping lipofuscin distribution in RPE, represents an indirect means of detecting, quantifying, and monitoring GA, it appears to be annoying and even painful for patients and dangerous for RPE and photoreceptors, maybe due to the potential deleterious effects related to photopigment consumption.[27] Moreover, cataract can affect FAF image quality more than CFP because the excitation wavelength is in the blue range of visible spectrum.[16]

Limitations of this study are related to the relatively small sample size and the large number of eyes excluded. The main reasons are poor FAF image quality resulting from cataract and the use of only lesions in which the area of GA was wholly contained within the raster scan area measuring $6 \times 6$ mm; however, fast and ongoing developments in OCT-A technology could allow for larger fields of view with higher resolution. Moreover, we cannot exclude influence by artifacts related to comparison between images obtained with different cameras.

In conclusion, thanks to the ability to image CC structure and flow impairments, OCT-A could be considered a reliable and appropriate technique for easily visualizing and quantifying GA and detecting foveal involvement. Although FAF imaging is currently considered the gold standard to identify GA and to evaluate treatment responses in ongoing clinical trials, we propose that, in the future, both in clinical settings and in clinical trials, OCT-A should be considered a useful tool for quantifying GA and monitoring the effect of therapies targeting GA progression.

## Acknowledgments

Disclosure: **E. Corbelli**, None; **R. Sacconi**, None; **A. Rabiolo**, None; **S. Mercuri**, None; **A. Carnevali**, None; **L. Querques**, None; **F. Bandello**, Alcon (C), Alimera Sciences (C), Allergan, Inc. (C), Farmila-Thea (C), Bayer Shering-Pharma (C), Bausch&Lomb (C), Genentech (C), Hoffmann-La-Roche (C), NovagaliPharma (C), Novartis (C), Sanofi-Aventis (C), Thrombogenics (C), Zeiss (C); **G. Querques**, Alimera Sciences (C), Allergan, Inc. (C), Heidelberg (C), Novaris (C), Bayer Shering-Pharma (C), Zeiss (C)

## References

1. Wong WL, Su X, Li X, et al. Global prevalence of age-related macular degeneration and disease burden projection for 2020 and 2040: a systematic review and meta-analysis. *Lancet Glob Health*. 2014;2:e106–e116.
2. Schatz H, McDonald HR. Atrophic macular degeneration. Rate of spread of geographic atrophy and visual loss. *Ophthalmology*. 1989;96:1541–1551.
3. Sunness JS, Rubin GS, Applegate CA, et al. Visual function abnormalities and prognosis in eyes with age-related geographic atrophy of the macula and good visual acuity. *Ophthalmology*. 1997;104:1677–1691.
4. Lindblad AS, Clemons TE. Responsiveness of the National Eye Institute Visual Function Questionnaire to progression to advanced age-related macular degeneration, vision loss, and lens opacity: AREDS Report no. 14. *Arch Ophthalmol*. 2005; 123:1207–1214.
5. Sunness JS, Margalit E, Srikumaran D. The long-term natural history of geographic atrophy from age-related macular degeneration: enlargement of atrophy and implications for interventional clinical trials. *Ophthalmology*. 2007;114:271–277.
6. Klein R, Meuer SM, Knudtson MD, Klein BE. The epidemiology of progression of pure geographic atrophy: the Beaver Dam Eye Study. *Am J Ophthalmol*. 2008;146:692–699.
7. Bartlett H, Eperjesi F. Use of fundus imaging in quantification of age-related macular change. *Surv Ophthalmol*. 2007;52: 655–671.
8. Holz FG, Bellman C, Staudt S, Schütt F, Völcker HE. Fundus autofluorescence and development of geographic atrophy in age-related macular degeneration. *Invest Ophthalmol Vis Sci*. 2001;42:1051–1056.

9. Holz FG, Bindewald-Wittich A, Fleckenstein M, Dreyhaupt J, Scholl HP, Schmitz-Valckenberg S; for the FAM-Study Group. Progression of geographic atrophy and impact of fundus autofluorescence patterns in age-related macular degeneration. *Am J Ophthalmol*. 2007;143:463–472.
10. Ben Moussa N, Georges A, Capuano V, Merle B, Souied EH, Querques G. MultiColor imaging in the evaluation of geographic atrophy due to age-related macular degeneration. *Br J Ophthalmol*. 2015;99:842–847.
11. Forte R, Querques G, Querques L, Leveziel N, Benhamou N, Souied EH. Multimodal evaluation of foveal sparing in patients with geographic atrophy due to age-related macular degeneration. *Retina*. 2013;33:482–489.
12. Sayegh RG, Simader C, Scheschy U, et al. A systematic comparison of spectral-domain optical coherence tomography and fundus autofluorescence in patients with geographic atrophy. *Ophthalmology*. 2011;118:1844–1851.
13. Pilotto E, Guidolin F, Convento E, et al. En face optical coherence tomography to detect and measure geographic atrophy. *Invest Ophthalmol Vis Sci*. 2015;56:8120–8124.
14. Waheed NK, Moult EM, Fujimoto JG, Rosenfeld PJ. Optical coherence tomography angiography of dry age-related macular degeneration. *Dev Ophthalmol*. 2016;56:91–100.
15. Kellner U, Kellner S, Weinitz S. Fundus autofluorescence (488 NM) and near-infrared autofluorescence (787 NM) visualize different retinal pigment epithelium alterations in patients with age-related macular degeneration. *Retina*. 2010;30:6–15.
16. Khanifar AA, Lederer DE, Ghodasra JH, et al. Comparison of color fundus photographs and fundus autofluorescence images in measuring geographic atrophy area. *Retina*. 2012; 32:1884–1891.
17. Yehoshua Z, Garcia Filho CA, Penha FM, et al. Comparison of geographic atrophy measurements from the OCT fundus image and the sub-RPE slab image. *Ophthalmic Surg Lasers Imaging Retina*. 2013;44:127–132.
18. Nunes RP, Gregori G, Yehoshua Z, et al. Predicting the progression of geographic atrophy in age-related macular degeneration with SD-OCT en face imaging of the outer retina. *Ophthalmic Surg Lasers Imaging Retina*. 2013;44: 344–359.
19. Yehoshua Z, de Amorim Garcia Filho CA, Nunes RP, et al. Comparison of geographic atrophy growth rates using different imaging modalities in the COMPLETE Study. *Ophthalmic Surg Lasers Imaging Retina*. 2015;46:413–422.
20. Rosenfeld PJ, Durbin MK, Roisman L, et al. ZEISS Angioplex™ spectral domain optical coherence tomography angiography: technical aspects. *Dev Ophthalmol*. 2016;56:18–29.
21. Pellegrini M, Acquistapace A, Oldani M, et al. Dark atrophy: an optical coherence tomography angiography study. *Ophthalmology*. 2016;123:1879–1886.
22. Cicinelli MV, Rabiolo A, Sacconi R, et al. Optical coherence tomography angiography in dry age-related macular degeneration [published online ahead of print June 22, 2017]. *Surv Ophthalmol*. doi:10.1016/j.survophthal.2017.06.005.
23. Sunness JS, Ziegler MD, Applegate CA. Issues in quantifying atrophic macular disease using retinal autofluorescence. *Retina*. 2006;26:666–672.
24. Querques G, Srour M, Massamba N, et al. Functional characterization and multimodal imaging of treatment-naïve "quiescent" choroidal neovascularization. *Invest Ophthalmol Vis Sci*. 2013;54:6886–6892.
25. Carnevali A, Cicinelli MV, Capuano V, et al. Optical coherence tomography angiography: a useful tool for diagnosis of treatment-naïve quiescent choroidal neovascularization. *Am J Ophthalmol*. 2016;169:189–198.
26. Capuano V, Miere A, Querques L, et al. Treatment-Naïve quiescent choroidal neovascularization in geographic atrophy secondary to non-exudative age-related macular degeneration. *Am J Ophthalmol*. 2017;182:45–55.
27. Tomasso L, Benatti L, Carnevali A, et al. Photobleaching by Spectralis fixation target. *JAMA Ophthalmol*. 2016;134:1060–1062.


Investigative Ophthalmology & Visual Science